applied sciences

MDPI

Article

Influence of Hot Carrier and Thermal Components on Photovoltage Formation across the p–n Junction

Jonas Gradauskas [1,2,*], Steponas Ašmontas [2], Algirdas Sužiedėlis [2], Aldis Šilėnas [2], Viktoras Vaičikauskas [2], Aurimas Čerškus [1,2], Edmundas Širmulis [2], Ovidijus Žalys [2] and Oleksandr Masalskyi [1]

[1] Department of Physics, Vilnius Gediminas Technical University, LT-10223 Vilnius, Lithuania; aurimas.cerskus@ftmc.lt (A.Č.); oleksandr.masalskyi@vgtu.lt (O.M.)

[2] Laboratory of Electronic Processes, Center for Physical Sciences and Technology, LT-10257 Vilnius, Lithuania; steponas.asmontas@ftmc.lt (S.A.); algirdas.suziedelis@ftmc.lt (A.S.); aldis.silenas@ftmc.lt (A.Š.); viktoras.vaicikauskas@ftmc.lt (V.V.); edmundas.sirmulis@ftmc.lt (E.Š.); ovidijus.zalys@ftmc.lt (O.Ž.)

* Correspondence: jonas.gradauskas@ftmc.lt; Tel.: +370-655-06220

Received: 6 October 2020; Accepted: 22 October 2020; Published: 24 October 2020

Abstract: In the present work we reveal the existence of the hot carrier photovoltage induced across a p–n junction in addition to the classical carrier generation-induced and thermalization-caused photovoltages. On the basis of the solution of the differential equation of the first-order linear time-invariant system, we propose a model enabling to disclose the pure value of each photovoltage component. The hot carrier photovoltage is fast since it is determined by the free carrier energy relaxation time (which is of the order of 10^{-12} s), while the thermal one, being conditioned by the junction temperature change, is relatively slow; and both of them have a sign opposite to that of the electron-hole pair generation-induced component. Simultaneous coexistence of the components is evidenced experimentally in GaAs p–n junction exposed to pulsed 1.06 μm laser light. The work is remarkable in two ways: first, it shows that creation of conditions unfavorable for the rise of hot carrier photovoltage might improve the efficiency of a single junction solar cell, and second, it should inspire the photovoltaic society to revise the Shockley–Queisser limit by taking into account the damaging impact of the hot carrier photovoltage.

Keywords: hot carriers; photovoltage; p–n junction; GaAs; solar cell

1. Introduction

Renewable energy such as an electric one generated by solar cells is a promising and environmentally friendly energy. To harvest it more extensively, one needs to reduce the production price of a solar cell and to increase its conversion efficiency. The conversion efficiency of a single p–n junction semiconductor solar cell is fundamentally constrained by the theoretical Shockley–Queisser limit [1]. In spite of multiple efforts (see, e.g., [2,3]) devoted to revise the limit, the theory assumes that only photons having energy close to a semiconductor forbidden energy gap E_g are used effectively, photons with energy below E_g are not absorbed at all (so called below E_g loss), and the residual energy of the higher energy photons left over after the electron-pair generation is reckoned only through the process of carrier thermalization, i.e., through the lattice heating (thermalization loss). These two intrinsic loss processes are mainly responsible for low efficiency of a single junction solar cell. For example, in a silicon cell, the below E_g loss amounts to 17% and the thermalization loss comes to 41%, and in a GaAs cell these both are equal to 34% and 26%, respectively [2].

Hot carriers (HCs) in semiconductors are free carriers with energy higher than the average one. The carriers can be heated by means of a DC electric field, microwave or optical radiation.

The photovoltaic community keeps a lively ongoing interest in hot carrier phenomena [4–11]. For good operation of a hot carrier solar cell, fast relaxation of carrier energy needs to be extended and the hot carriers need to be extracted through the selective contacts before they cool down to the bandgap edges. Despite the advances in theory and materials synthesis, practically hot carrier solar cell remains unrealized.

One way of experimental detection of carrier heating can be implemented by laser radiation with photons having energy lower than a semiconductor forbidden energy gap. Such intraband light absorption initiates rise of the hot carrier photovoltage across a semiconductor potential barrier (Figure 1a; process 2). This kind of photoresponse was investigated in Ge [12], Si [13] and GaAs [14] l-h junctions illuminated with CO_2 laser radiation (photon energy 0.12 eV). It was shown [14] that the photovoltage consisted of two components, the slow and the fast one. The fast one was attributed to the HC photoresponse, while the slow one was assumed to result from the semiconductor lattice heating, i.e., from the carrier thermalization. Actually, the process of thermalization is also based on the hot carrier phenomenon since the hot carriers supply the lattice with this extra energy while cooling down to the bandgap edges. Low photon energy laser pulses also gave rise to HC photovoltage across Ge [15], Si [16,17], GaAs [18–20], InSb [21] and HgCdTe [22] p–n junctions. It is worth noting that in the case of the narrow bandgap semiconductors (InSb and HgCdTe) exposed to the CO_2 laser light pulses, the classical photovoltage induced by electron-hole pair generation was observed simultaneously with the HC photoresponse. Additionally, both these photovoltages were observed across Si p–n junction illuminated with 1.49 μm-long laser radiation [19] and across GaAs p–n junction exposed to 1.06 μm wavelength light [19,20]. The polarities of these two photovoltages are opposite.

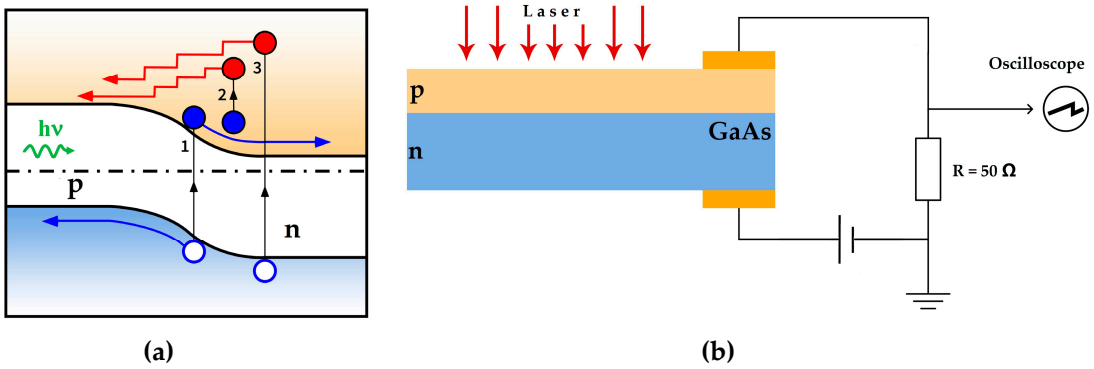

Figure 1. (**a**) Formation of generation-induced photovoltage (blue arrows) and hot carrier photovoltage (red arrows) across the p–n junction; stepped shape of the red arrows indicates gradual thermalization of a hot carrier. 1—process of electron-hole pair generation, 2—free electron heating and 3—generation of hole and hot electron pair; (**b**) schematic of the sample and photovoltage measurement circuit.

High-energy photons also create hot carriers as the excess energy turns the photogenerated carriers into the hot ones [20,23], and these show a two-sided influence on the open circuit voltage of a p–n junction [23].

This paper deals with all three effects, i.e., hot carriers, thermalization and classical photogeneration, simultaneously induced by a laser pulse across the GaAs p–n junction. We propose a method unfolding the input of each individual component into the net magnitude of the photoresponse and focus our interest on the hot carrier photovoltage as a possible reason for the practically unattainable theoretical Shockley–Queisser limit.

2. Experimental

The object of our investigation, GaAs p–n junction, was fabricated from 5 μm-thick p-type layer (hole density 5×10^{17} cm^{-3}) liquid phase epitaxy-grown on n-type substrate with electron density 3×10^{17} cm^{-3}. Traditional photolithography technique and thermal evaporation of the Au-Ge-Ni alloy

were applied to form the 2.5 × 2.5 mm^2 sample with ohmic contacts. The contacts were built at the edge of the sample to prevent them from a direct laser beam and thus to avoid photosignal formation in the vicinity of the contacts (Figure 1b).

A laser is a useful tool to investigate the hot carrier phenomena for its unique features of monochromatic and wide power range emission and for the possibility of generating short light pulses. In the experiment, Nd:YAG laser with wavelength 1.06 μm, pulse duration 25 ns, repetition rate 50 Hz and maximum pulse intensity 1.2 MW/cm^2 was used. The measurement scheme is also presented in Figure 1b. Temporal behavior of the photovoltage and laser pulse shapes was recorded by digital storage oscilloscope Agilent Technologies DSO6102A, and the laser pulse shape was registered by high speed optical signal reference detector 11HSP-FS1 (Standa Ltd., Vilnius, Lithuania). The calculations were performed by means of multi-paradigm numerical computing environment MATLAB (R2019b, The MathWorks, Natick, MA, USA, 2019).

3. Results

Figure 2a presents oscilloscope trace of the photovoltage across the GaAs p–n junction induced by the laser pulse at 20% of its maximum intensity value. It is seen that the response consisted of at least two components of opposite polarity. The positive one corresponded to electron-hole pair generation and their separation by the electric field of the junction (process 1 in Figure 1a). Additionally, the negative part obviously agreed with the carrier flow above the potential barrier (red arrows in Figure 1a), i.e., it could be attributed to the hot carrier photovoltage.

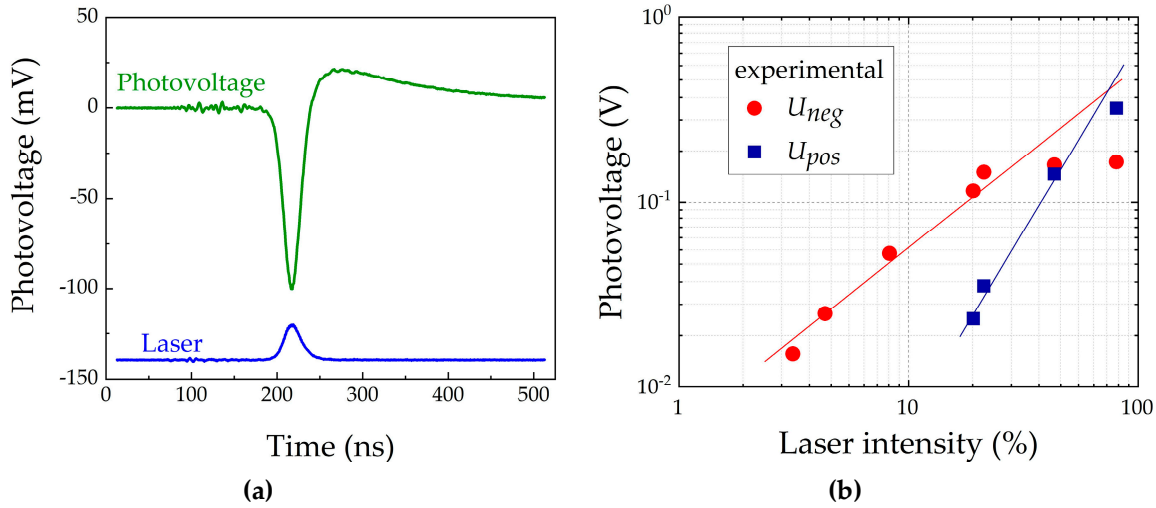

Figure 2. (**a**) Experimental photovoltage signal (green) across GaAs p–n junction at the moderate light intensity level; laser pulse (blue) is added for time-dependent comparison. (**b**) Dependence of measured peak values of the negative U_{neg} (red circles) and positive U_{pos} (blue squares) photovoltage components on laser light intensity; the lines are guides for the eye of linear (red) and square law (blue) dependence.

The laser photon energy was less than the forbidden energy gap of GaAs, $h\nu$ = 1.17 eV and E_g = 1.42 eV, respectively. Thus, the intraband light absorption could be the reason of the hot carrier photovoltage formation as it took place in the case of CO_2 laser excitation [18]. On the other hand, GaAs is known for its relatively expressed two-photon absorption [24]. This feature can be assumed to be the reason of the carrier pair generation-caused photovoltage formation. Really, the measured peak value of the negative component U_{neg} shows linear dependence on the laser intensity (red circles in Figure 2b); this is an inherent feature of the heating-caused effects. While the positive component U_{pos} followed the square law thus proving its origin to be related with the mechanism of two-photon absorption (blue squares in Figure 2b).

Moreover, the presence of hot carriers was unavoidably followed by their fast thermalization and resulting rise of the junction temperature. Therefore, the total photoresponse across the GaAs p–n junction should be composed of three components,

$$U_{tot}(t) = U_{hc}(t) + U_{th}(t) + U_{gen}(t), \quad (1)$$

where $U_{hc}(t)$ is the hot carrier photovoltage, $U_{th}(t)$ is the thermal component resulting from thermalization of hot carriers and subsequent heating of the lattice and $U_{gen}(t)$ is the electron-hole pair generation-based component arising due to two-photon absorption. The polarities of $U_{hc}(t)$ and $U_{th}(t)$ were the same and were opposite to the sign of $U_{gen}(t)$. Our model assumed the p–n junction as a first-order linear time-invariant (LTI) system [25], and the time-response of it in a general case was characterized by the differential equation

$$\tau \frac{dU}{dt} + U = \overline{U}(t), \quad (2)$$

where τ represents the exponential decay constant, and $U = U(t)$ is a photoresponse function of time. The forcing function $\overline{U}(t)$ depends on the laser pulse and on the physical phenomenon giving rise to a particular photoresponse component. In our case, the laser pulse can be properly approximated as

$$I(t) = I_p \left(\frac{t}{\tau_p}\right)^m exp\left[m\left(1 - \frac{t}{\tau_p}\right)\right], \quad (3)$$

where I_p is the peak intensity, $I_p = I(\tau_p)$ and τ_p is the laser pulse rise time. The best fit with the experimental laser pulse shape was achieved with index $m = 10$.

As it was mentioned earlier, generation of electron-hole pairs was caused by a nonlinear phenomenon of two-photon absorption. Therefore, the forcing function has a square dependence on the laser intensity:

$$\overline{U}_{gen}(t) = K_{gen} I^2(t). \quad (4)$$

To solve Equation (2) in respect to $U_{gen}(t)$, the time constant τ_{gen} was measured as the exponential decay of the positive component, and the coefficient K_{gen} was chosen to fit the experimental photovoltage magnitude far after the end of the laser pulse. The calculated $U_{gen}(t)$ is presented in Figure 3a in green. Additionally, the experimental trace of the total photovoltage is depicted here. As expected, good agreement was seen only at the end of the picture.

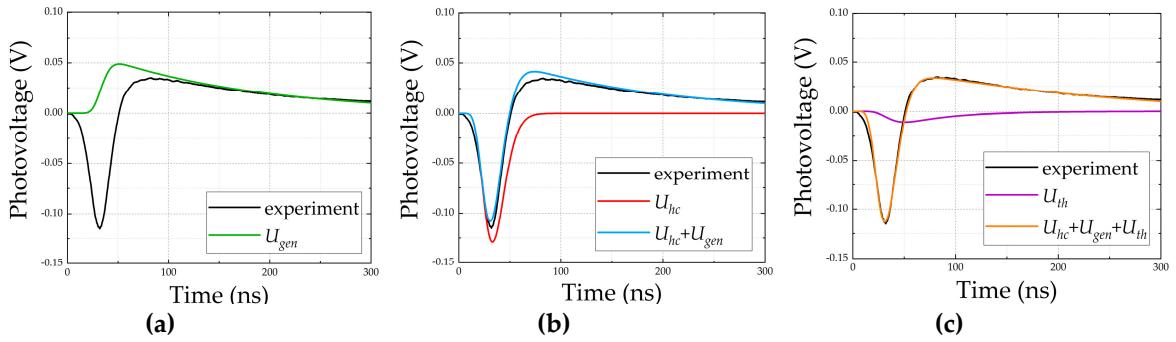

Figure 3. Sequence of photovoltage pulse simulation: (**a**) carrier generation-induced component (green); (**b**) hot carrier photovoltage (red) and sum of the two components (blue) and (**c**) thermal lattice heating-caused photovoltage (violet) and sum of the three components (orange). For comparison, the experimental photovoltage trace is shown in black.

Hot carrier energy relaxation time in GaAs is of the order of one picosecond [26]. It means that the free carriers are hot as long as the laser pulse is present:

$$\overline{U}_{hc}(t) = K_{hc}\, I(t), \tag{5}$$

and the time constant is $\tau_{hc} = \tau_p$. The value of coefficient K_{hc} was tailored to fit $U_{hc}(t)$ with the negative peak of the experimental trace. The hot carrier component $U_{hc}(t)$ and the sum of the two calculated components, $U_{hc}(t) + U_{gen}(t)$, are presented in Figure 3b. Obviously, to reach better congruence with the measured photovoltage, one needs a slow negative component to be added to the calculated binary trace.

Heating effects, no matter whether they are of the free carriers or of a semiconductor lattice, are linear phenomena. Thus, the forcing function of the thermalization-caused component is expressed as

$$\overline{U}_{th}(t) = K_{th}\, I(t). \tag{6}$$

For calculation of $U_{th}(t)$, the value of τ_{th} = 160 ns was estimated by measuring the time-decay of the transient thermoelectric (TTE) voltage [27] between two contacts on the sample's substrate exposed to the laser radiation. The magnitude of K_{th} was tailored for the best fitting of the calculated and experimental results.

As Figure 3c shows, addition of the third, thermal, component (violet trace) improved the proposed model and gave good agreement with the experimental data. Thus, the model is provided with an ability to separate all the components and to evaluate the contribution of each of them to the total photovoltage. The dependence of the peak values of all three derived components, $U_{gen}(t)$, $U_{hc}(t)$ and $U_{th}(t)$, on laser intensity are depicted in Figure 4. Each point was calculated by applying the above model for each photovoltage trace experimentally fixed at the appropriate laser intensity level.

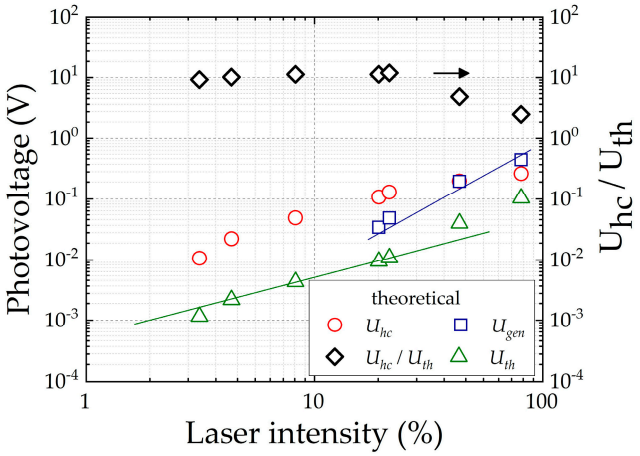

Figure 4. Simulated photovoltage components versus light intensity: the hot carrier U_{hc} in red circles, the generation-caused U_{gen} in blue squares and the thermal one U_{th} in green triangles. The calculated ratio U_{hc}/U_{th} is shown in black diamonds. The lines are guides for the eye of linear (green) and square law (blue) dependence.

As the laser intensity increased and the two-photon absorption started to be detected (at approximately about 20% of the maximum intensity value), several notices should be pointed out. First, the magnitude of the measured U_{gen} was lower than the modeled one (compare the values in Figures 2b and 4). It confirms that the classical photovoltage across the p–n junction was lowered by the opposing heating effects. Second, the dependence of the U_{hc} component passed into the sublinear character, that is, its input into the total signal seemed to diminish. This must be caused by the relative lack of light photons directly used for the carrier heating since part of them now was used for the carrier generation. Third, the interplay between the measured and calculated U_{hc} component peak values

also changed: the experimental one led at low laser intensities while it gave place to the calculated one at the higher excitation level. Influence of the other two components was responsible for these changes: U_{th} supported the experimental U_{hc} at low intensities (see cases b and c in Figure 3), and U_{gen} cut down U_{hc} as it started manifesting itself. Fourth, the input of the slow lattice heating-caused component U_{th} seemed to increase since it went into the superlinear shape. Actually, it was not the real case. Part of the energy remaining from the electron-hole generation due to two-photon absorption ($2 \times h\nu - E_g = 0.92$ eV) was most probably used to generate a hot carrier, which supported formation of the hot carrier photovoltage (Figure 1a, process 3). However, this process followed the slow temporal behavior of the U_{gen} as both of them did happen at the same time and therefore could not be separated. Therefore, the decrease of the ratio U_{hc}/U_{th} (black diamonds in Figure 4) should be treated as the relative decrease of that HC component, which resulted only from direct intraband free carrier absorption. Nevertheless, one should note a ten times stronger impact of the hot carriers as compared to that of the heated lattice at low light intensity.

It is well known that bias voltage alters the potential barrier height and the depleted region of a p–n junction. Thus, forward bias should set favorable conditions for the hot carrier flow across the lowered potential barrier (see Figure 1a). Indeed, the experiment shows that the negative fast photovoltage component increased with the forward bias voltage and decreased with the reverse one (Figure 5). As process 1 in Figure 1a illustrates, a p–n junction solar cell got forwardly biased by the electron-hole pairs generated and separated by the internal electric field what should work for the good of the damaging impact of the hot carriers on the cell operation. However, in the case of the reverse-biased junction, sharp drop of the magnitude of the fast component is seen in the region of light intensity when the carrier generation-induced component met favorable conditions and started manifesting itself (Figure 5, at above 5% of maximum intensity value); the rise of the latter was well-seen in the inset at U < 0. This way, correlation between the hot carrier-induced photovoltage and the generation-caused one was ambiguous, but the opposition between these two photovoltages was obvious.

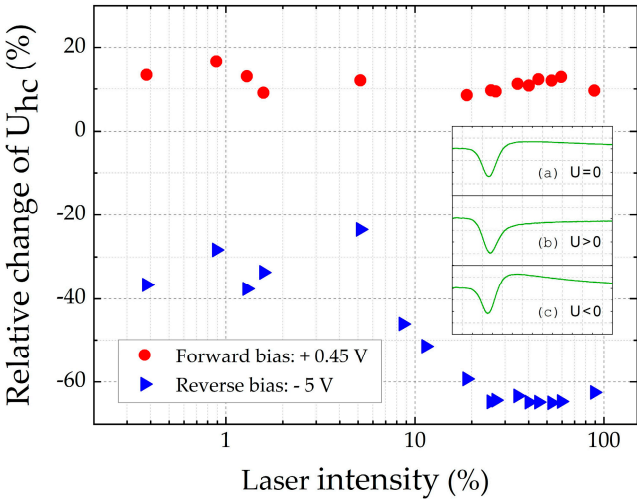

Figure 5. Dependence of the relative change of the hot carrier photovoltage ($U_{hc}{}^{biased} - U_{hc}{}^{nonbiased}$)/$U_{hc}{}^{nonbiased}$ on laser light intensity at +0.45 V forward bias voltage (red circles) and −5 V reverse bias (blue triangles). In inset: typical experimental photovoltage pulse traces at zero (**a**), forward (**b**) and reverse (**c**) bias voltage; the scale is 50 mV/div and 50 ns/div.

4. Conclusions

Hot carrier photovoltage across the GaAs p–n junction was evidenced experimentally and supported by an empirical model. In general, photovoltage across a p–n junction consisted of three simultaneous components arising due to electron-hole pair generation, hot carrier effect and

semiconductor lattice heating after the thermalization. The first two of them could be evaluated experimentally at some extent, while the lattice heating-caused component could not be detected separately. The proposed model of a p–n junction as a first-order LTI system allowed revealing the individual input of each component. The magnitude of the net photovoltage resulted from mutual competition between all three components. Under certain conditions, depending on light wavelength, intensity, semiconductor bandgap and bias voltage, the hot carrier component could even exceed the classical photovoltage. As for application, the hot carrier photovoltage might be the reason of the still experimentally unattainable Shockley–Queisser limit, and the so called below E_g loss should be revised by taking into account the formation of this photovoltage of opposite polarity. On the other hand, maximum reduction of the hot carrier photovoltage contribution will boost the efficiency of a single-junction solar cell.

Author Contributions: Conceptualization and methodology, S.A. and J.G.; sample fabrication, A.Š. and A.S; formal analysis, V.V. and A.Č.; experimental investigation, E.Š., O.Ž and O.M.; calculations, O.M.; writing, reviewing and editing, J.G., S.A. and A.S.; visualization, O.Ž. and O.M.; project administration and supervision, S.A. All authors have read and agreed to the published version of the manuscript.

Funding: This work was in part supported by the Research Council of Lithuania (grant No. 01.2.2-LMT-K-718-01-0050).

Conflicts of Interest: The authors declare no conflict of interest. Additionally, the funders had no role in the design of the study; in the collection, analyses, or interpretation of data; in the writing of the manuscript, or in the decision to publish the results.

References

1. Shockley, W.; Queisser, H. Detailed Balance Limit of Efficiency of p–n Junction Solar Cells. *J. Appl. Phys.* **1961**, *32*, 510–519. [CrossRef]
2. Hirst, L.C.; Ekins-Daukes, N.J. Fundamental losses in solar cells. *Prog. Photovolt. Res. Appl.* **2011**, *19*, 286–293. [CrossRef]
3. Ruhle, S. Tabulated values of the Shockley–Queisser limit for single junction solar cells. *Sol. Energy* **2016**, *130*, 139–147. [CrossRef]
4. Nelson, C.A.; Monahan, N.R.; Zhu, X.-Y. Exceeding the Shockley–Queisser limit in solar energy conversion. *Energy Environ. Sci.* **2013**, *6*, 3508–3519. [CrossRef]
5. Goodnick, S.; Honsberg, C. Modeling carrier relaxation in hot carrier solar cells. In Proceedings of the Physics, Simulation, and Photonic Engineering of Photovoltaic Devices, San Francisco, CA, USA, 23–26 January 2012; pp. 82560W-0–82560W-10.
6. Konovalov, I.; Plos, B. Modeling of hot carrier solar cell with semi-infinite energy filtering. *Sol. Energy* **2019**, *185*, 59–63. [CrossRef]
7. Hirst, L.C.; Fujii, H.; Wang, Y.; Sugiyama, M.; Ekins-Daukes, N.J. Hot carriers in quantum wells for photovoltaic efficiency enhancement. *IEEE J. Photovoltaics* **2014**, *4*, 244–252. [CrossRef]
8. Tsai, C.-Y. Theoretical model and simulation of carrier heating with effects of nonequilibrium hot phonons in semiconductor photovoltaic devices. *Prog. Photovolt. Res. Appl.* **2018**, *26*, 1–17. [CrossRef]
9. Hirst, L.C.; Walters, R.J.; Fuhrer, M.F.; Ekins-Daukes, N.J. Experimental demonstration of hot-carrier photo-current in an InGaAs quantum well solar cell. *Appl. Phys. Lett.* **2014**, *104*, 231115–231119. [CrossRef]
10. Kamide, K. Current–voltage curves and operational stability in hot-carrier solar cell. *J. Appl. Phys.* **2020**, *127*, 183102–183118. [CrossRef]
11. Wang, G.; Liao, L.P.; Elseman, A.M.; Yao, Y.Q.; Lin, C.Y.; Hu, W.; Liu, D.B.; Xu, C.Y.; Zhou, G.D.; Li, P.; et al. An internally photoemitted hot carrier solar cell based on organic-inorganic perovskite. *Nano Energy* **2020**, *68*, 104327–104383. [CrossRef]
12. Ašmontas, S.; Gradauskas, J.; Seliuta, D.; Sužiedėlis, A.; Valušis, G.; Širmulis, E. Fast infrared detectors based on nonuniform semiconductors. In Proceedings of the Advanced Optical Devices, Technologies, and Medical Applications, Bellingham, WA, USA, 18–22 August 2003; pp. 221–230.
13. Ašmontas, S.; Maldutis, E.; Širmulis, E. CO_2 Laser radiation detection by carrier heating in inhomogeneous semiconductors. *Int. J. Optoelectron.* **1988**, *3*, 263–266.

14. Ašmontas, S.P.; Gradauskas, J.; Seliuta, D.; Širmulis, E. Photoresponse in nonuniform semiconductor junctions under infrared laser excitation. In Proceedings of the Fourth International Conference on Material Science and Material Properties for Infrared Optoelectronics, Kiev, Ukraine, 29 September–2 October 1998; pp. 125–131.
15. Umeno, M.; Sugito, Y.; Jimbo, T.; Hattori, H.; Amenixa, Y. Hot photo-carrier and hot electron effects in p-n junctions. *Sol. St. Electron.* **1978**, *21*, 191–195. [CrossRef]
16. Andrianov, A.V.; Valov, P.M.; Sukhanov, V.L.; Tuchkevich, V.V.; Shmidt, N.M. Photoeffect on silicon p–n junction under intraband carriers heating by light. *Phys. Techn. Poluprovodn.* **1980**, *14*, 859–864.
17. Encinas-Sanz, F.; Guerra, J.M. Laser-induced hot carrier photovoltaic effects in semiconductor junctions. *Prog. Quantum Electron.* **2003**, *27*, 267–294. [CrossRef]
18. Ašmontas, S.; Gradauskas, J.; Seliuta, D.; Širmulis, E. Photoelectrical properties of nonuniform semiconductor under infrared laser radiation. In Proceedings of the Nonresonant Laser-Matter Interaction (NLMI-10), St. Petersburg, Russia, 21–23 August 2000; pp. 18–27.
19. Ašmontas, S.; Gradauskas, J.; Sužiedėlis, A.; Šilėnas, A.; Širmulis, E.; Švedas, V.; Vaičikauskas, V.; Vaičiūnas, V.; Valiulis, D.; Žalys, O.; et al. Peculiarities of photovoltage formation across p-n junction under illumination of laser radiation. *Solid State Phenom.* **2017**, *267*, 167–171.
20. Ašmontas, S.; Gradauskas, J.; Sužiedėlis, A.; Šilėnas, A.; Širmulis, E.; Švedas, V.; Vaičikauskas, V.; Žalys, O. Hot carrier impact on photovoltage formation in solar cells. *Appl. Phys. Lett.* **2018**, *113*, 071103–071106. [CrossRef]
21. Ašmontas, S.; Gradauskas, J.; Naudjyus, K.; Širmulis, E. Photoresponse of InSb-based p-n structures during illumination by a CO_2 laser. *Semiconductors* **1994**, *28*, 1089–1091.
22. Ašmontas, S.; Gradauskas, J.; Seliuta, D.; Sužiedėlis, A.; Širmulis, E.; Valušis, G.; Tetyorkin, V.V. CO_2 Laser Induced Hot Carrier Photoeffect in HgCdTe. *Mater. Sci. Forum* **2002**, *384–385*, 147–150.
23. Kempa, K.; Naughton, M.J.; Ren, Z.F.; Herczynski, A.; Kirkpatrick, T.; Rybczynski, J.; Gao, Y. Hot electron effect in nanoscopically thin photovoltaic junctions. *Appl. Phys. Lett.* **2009**, *95*, 233121–2331214. [CrossRef]
24. Hurlbut, W.C.; Lee, Y.-S.; Vodopyanov, K.L.; Kuo, P.S.; Fejer, M.M. Multiphoton absorption and nonlinear refraction of GaAs in the mid-infrared. *Opt. Lett.* **2007**, *32*, 668–670. [CrossRef]
25. Won, W.; Yang, Y.; Chang, T.G.; Song, I.H.; Cho, Y.S.; Heo, J.; Jeon, W.G.; Lee, J.W.; Kim, J.K. Input-Output Relationship of LinearTime-Invariant (LTI) System. In *Signals and Systems with MATLAB*; Springer: Berlin/Heidelberg, Germany, 2009; pp. 15–17.
26. Glover, G.H. Study of electron energy relaxation times in GaAs and InP. *J. Appl. Phys.* **1973**, *44*, 1295–1301. [CrossRef]
27. Sasaki, M.; Negishi, H.; Inoue, M. Pulsed laser–induced transient thermoelectric effects in silicon crystals. *J. Appl. Phys.* **1986**, *59*, 796–802. [CrossRef]

Publisher's Note: MDPI stays neutral with regard to jurisdictional claims in published maps and institutional affiliations.

© 2020 by the authors. Licensee MDPI, Basel, Switzerland. This article is an open access article distributed under the terms and conditions of the Creative Commons Attribution (CC BY) license (http://creativecommons.org/licenses/by/4.0/).